Chapter 6
Assessment of Climate Change Impacts on Urban Rainfall Extremes for Achieving Sustainable Urban Water Development in Hanoi, Vietnam

Binaya Kumar Mishra, Chitresh Saraswat, Linh Nhat Luu, Thuc Tran, Khiem Van Mai, Shamik Chakraborty, and Pankaj Kumar

Abstract In recent decades, the increased frequency of disaster events, particularly hydro-meteorological disasters, have threatened human lives and infrastructure. In the context of climate change, urban water management became more complicated because of erratic or heavy rain events or prolonged droughts. Now, sustainable water management and planning requires to visualize the potential impact of climate change on extreme rainfall pattern in order to reduce the climatic vulnerability. This chapter evaluates the impact of climate change on extreme rainfall intensities under different greenhouse gases emission RCP (Representative Concentration Paths) considering future period of 2070–2099 over a baseline period of 1976–2005. The impacts were assessed using rainfall output of 5 General Circulation Models (GCM) under RCP 8.5 (high) and RCP 4.5 (medium) emission scenarios. Bilinear interpolation and quantile mapping technique were applied to extract rainfall data from grid points onto station points and to correct bias of GCM simulations in comparison with the observational data respectively. To derive the rainfall IDF (Intensity-Duration-Frequency) curves, daily rainfall output was temporally downscaled using scaling method. In the study, IDF curves were developed and the performances of the downscaling method were evaluated. The results indicate that the mean of corrected monthly rainfall and the frequency of wet days are considerably closer to observation than the raw rainfall estimates. In addition, the bias correction method accurately captured extreme rainfall values for all 5 GCM

B. K. Mishra · S. Chakraborty · P. Kumar
Institute for the Advanced Study of Sustainability, United Nations University, Tokyo, Japan

C. Saraswat (✉)
Institute for the Advanced Study of Sustainability, United Nations University, Tokyo, Japan

Graduate School of Global Environmental Science, Sophia University, Tokyo, Japan

L. N. Luu · T. Tran · K. Van Mai
Institute of Meteorology, Hydrology and Environment, Hanoi, Vietnam

G. Huang, Z. Shen (eds.), *Urban Planning and Water-related Disaster Management*, Strategies for Sustainability,
https://doi.org/10.1007/978-3-319-90173-2_6

and indicated that by the end of the century, under different scenarios the rainfall intensity is increasing for all the durations and the return periods. The results will assist the water manager and urban planner to design the sustainable and robust water infrastructure.

Keywords Urban water planning · Sustainable water management · Rainfall IDF · Climate change · Bias correction · Downlscaling

6.1 Introduction

Water is a basic necessity and valuable resource that needs to be managed and used sensibly, which is gradually transforming into a crisis that is responsible for a bad health condition, destroying livelihoods for many and inflicting unnecessary suffering for poor (Connor 2015; Hanjra and Qureshi 2010). It is one of the biggest challenges our generation is facing (IPCC 2014). To overcome this crisis, development of clean potable water, managing wastewater efficiently, providing basic sanitation facilities, developing robust water management in both urban and rural areas and integrating sustainability in our daily life is necessary to achieve water sustainability (Conca 2006; UNEP 2012; Tremblay 2010). Specially the condition is deteriorating in urban areas, where industrialization, growing human population, and urbanization exerting a significant amount of pressure on the water bodies that keep ecosystems flourishing and nourished. In urban region around the world, the water systems such as rivers, lakes, ponds and, aquifers are drying up due to changes in climate or pollution due to anthropogenic activities (Saraswat and Kumar 2016; Saraswat et al. 2016). The climate change is altering the patterns of water cycle along with the weather, which is causing floods in some region and droughts in others at the same time. The climate change has been described as the significant changes in the weather patterns, temperature, precipitation (intensity, frequency and duration) and several others (Saraswat et al. 2017; USEPA 2015). In year 2014, the IPCC assessment report analyzed that the intense rainfall events are seen worldwide and the number of such events increased, particularly on land regions, which induced heavy discharge in catchments (IPCC 2014). The heavy discharge can lead to greater risks of flooding at a regional scale and national scale (IPCC 2014). It is recognized by IPCC that the water-related issues such as flooding and water scarcity is major issues to deal with in the twenty-first century (Adusumalli and Arora 2015). It is also expected that 60–70% of the world's population may even face water scarcity due to the increasing trend of climate change and urbanization (UNDESA 2016).

Most of the time, due to communication and coordination inefficiencies of system urban planners and water manager unable to coordinate effectively on designing of approaches, results in disaster for sustainable urban planning. In this chapter, we argue that the assessment of climate change impact on rainfall IDF (Intensity-Duration-Frequency) curves will be helpful and support urban water management, which should be an integral part of sustainable urban development and planning. Flood risk in urban area is a serious challenge for an effective urban planning and

development. Recently, the approaches to urban water management and flood risk control have been changed from "hard measures" to more "integrated management" measures such integration of stormwater management, rainwater harvesting, structural development and also 'soft' measures all together, in which ecosystem services for flood regulation play an important role (Mishra et al. 2017; Mai and Herath 2014). In urban regions, the rapid and unplanned urbanization is one of the major thrusts for deteriorating urban water management and water security (Mishra et al. 2017; Saraswat et al. 2017). Urbanization leads to the creation of impervious surfaces, which lead to an increase in surface runoff volume and contributes to downstream flooding (Saraswat et al. 2016; Yan et al. 2015), eventually, the loss of recharge affects residential and municipal water supplies. Due to this the environmental problems such as clean water provision, wastewater production, and treatment as well as disasters such as flooding and land subsidence, have become commons in many cities (Mishra et al. 2017; Jago-on et al. 2009). In many urban areas, the sustainable use of water is approaching or exceeding the limits (Mishra et al. 2017; Hatt et al. 2007).

River basins also comprise complex-adaptive systems, and the socio-ecology of rivers needs particular attention for an integrated management (Chakraborty and Chaktraborty 2017). There is a need to carry out management of the freshwater landscapes through the biotic elements the freshwater systems possess, especially so, as it is an often 'forgotten' aspect of water resource management. These biotic elements should not be 'synthetic', that is, brought in as a quick fix solution for restoration, but should (ideally) be a part of the natural succession of the freshwater systems. It is high time that the urban areas as well as rural areas surrounding urban areas incorporate biotic elements as 'indicators' of healthy freshwater environments. These cases also strongly suggest that a biospheric understanding rather than a (scientific) approach that tries to synthetize nature (through, for example, water purification) can be a better solution for sustainable water environments in the urban areas. The importance of rural-urban linkage is no less important feature here as freshwater environments such as rivers and streams pass through irrespective of these landscapes. Also, the rural environments upstream serve as part of the urban watershed and affected by urban land use, creating rivers whose biospheric components are greatly compromised. The example of Lake Kasumigaura near Tokyo, Japan can be raised in this regard. Kasumigaura is a shallow lake (with average depth of about 4 m) with healthy fisheries until around 1970s, when large scale concretization of bed and banks of the Lake and its tributary rivers caused the aquatic vegetation to decrease, with resultant increase in the pollution level of the lake. This is another instant where not accounting the biological properties of the water landscapes has caused a big problem for the lake's fisheries. The restoration of Kasumigaura with water purification technology has yielded no result and the lake continues to have deterioration in its water quality, with noted eutrophication events. This led to decrease of native and traditional fisheries like smelt harvest and reduce the fisheries to introduced species only (Takeuchi et al. 2003). Nymphoides peltata or Asaza is vegetation that is especially suffered from the concretization of the bed and banks of the lake and rivers around Kasumigaura (ibid). It is another biotic agent that can show the 'health' of the water landscape. The case suggests that

biotic components of the freshwater system in question are a viable way to achieve the integrated management.

This research is addressing the challenge of extensive urban floods due to an increase of rainfall intensities in urban areas brought about by climate change (Pereira et al. 2009). Due to climate change, the water resources will be affected in both quantity and quality, and hence water, stormwater, and wastewater facilities infrastructure and urban water management will face a greater risk of damage (Saraswat et al. 2016). Therefore, to achieve sustainable water management, it is important to quantify and visualize the climate change impacts on urban water infrastructure, which is expected to deteriorate water management by altering rainfall patterns (Saraswat et al. 2017). The result will be more floods in the rainy season and water scarcity in dry season. Recently, it has been observed that the frequency of natural disaster events is increasing, particularly hydro-meteorological disasters which, directly threatened the human lives, economies and infrastructure. In the context of climate change, water management is becoming more complicated because of erratic or heavy precipitation, rainfall events or prolonged droughts (Yilmaz et al. 2014). Sustainable water management and planning requires the quantifying the potential effects of climate change on extreme rainfall pattern to help in reducing the climatic vulnerability. Specially, change in spatial and temporal distribution of extreme rainfall events in future need to be precisely understood in preparing urban drainage master plans which include design of stormwater drains in the city, bigger storage in the upper region, river bank wall, channel widening and and many other structures involving hydrologic flows (Westra et al. 2014; Prodanovic and Simonovic 2007; et al. 2012).

Rainfall intensity-duration-frequency (IDF) curve presents the probability of a given rainfall intensity and duration expected to occur at a particular location. The rainfall IDF, which was first introduced by Bernard in 1932, is widely used by water scientists and civil engineers during planning and design of various hydraulic strucutres. Design standards for considering specific return period values depend on type of water infrastructure as well as their location. Climate change is widely projected to increase frequency and intensity of extrme rainfall events resulting larger design rainfall value in the future for the same return period. Thus, conventional (stationary) frequency analysis method of estimating extreme rainfall will be inadequate and require revision of existing guidelines and standards to accommodate higher value of rainfall in planning and designing various hydraulic infrastructures. In this case, the rainfall IDF relationships may be used advantageously for urban water management and planning. De Paola et al. (2014) estimated the rainfall IDF for three cities, including Addis Ababa (Ethiopia), Dar Es Salaam (Tanzania) and Douala (Cameroon), using rainfall observations and rainfall estimates derived from the CMCC (Centro Euro-Mediterraneo sui Cambiamenti Climatici) model. The temporal disaggregation method was used to obtain the rainfall amounts over smaller time scale. The evaluation of rainfall IDF was conducted and then the projection of rainfall IDF was estimated to verify the change of extreme values under climate change. Akpan and Okoro (2013) developed two sets of rainfall IDF models for the Calabar City (Nigeria), and estimated the relationship between rainfall intensity and duration for specific frequencies and associated rainfall intensity and frequency for

specific durations, using a rainfall dataset from 2000 to 2009. These models are used to predict the possibility of a certain amount of rainfall that may be used in planning and designing of the infrastructure in Nigeria. Logah et al. (2013) analyzed rainfall data of four stations in Greater Accra Region to develop the rainfall intensity – duration – frequency curves by fitting the rainfall intensity to Gumbel distribution for various durations. Le et al. (2006) used 4 empirical functions including the Talbot, Bernard, Kimijima and Sherman equations to construct rainfall IDFs for several stations in Vietnam. Their study compared the results between these 4 methods and then chose the appropriate equation for Vietnam. In addition, their study also proposed a method to generalize the IDF curve for ungauged rainfall locations over Vietnam. Wang et al. (2014) applied PRECIS regional climate model for investigating the potential impact of climate change on rainfall IDF over Ontario, Canada. Their results reported that all rainfall extreme events for different durations and return periods return periods are likely to increase over 2030s, 2050s and 2080s.

Nguyen et al. (2007) constructed rainfall IDF curves using temporally and spatially downscaled rainfall data under the A2 scenario. In their study, SDSM (Statistical DownScaling Model) method combined with bias correction was employed to obtain adjusted daily rainfall estimates at several rain gauge stations in Quebec. Later, using scaling method, sub-daily rainfall values were produced by applying Generalized Extreme Value (GEV) distribution on daily data. Rodríguez et al. (2014) studied the impact of climate change on rainfall IDF over Barcelona (Spain). This change was analyzed from the output of five General Circulation Models (GCM) under three scenarios, including A1B, A2 and B2. Willems and Vrac (2011) took into account the change of rainfall IDF for Belgium based on several rainfall data series. The results indicated that the increase in extreme rainfall could be 30% by the end of the century. In recent climate change impact studies, use of quantile mapping technique is widely popular for minimizing biases in the GCM rainfall output. In this technique, observation and GCM rainfall data of past period (usually 30 years) are compared and checked for any significant biases in their values (Hansen et al. 2007; Mpelasoka and Chiew 2009; Kuo et al. 2015). Accordingly, differences in statistics like mean rainfall, maximum rainfall and number of rainy (wet) days and rainfall over the study period are estimated and corrected future GCM is obtained. Mishra and Herath (2014) applied quantile mapping technique to correct biases in MRI-GCM (Meteorological research Institute) rainfall for the assessment of climate change impact on flood-frequency in the Bagmati river basin, Nepal. Mirhosseini et al. (2012) applied scaling factor to correct the GCM output by comparing monthly rainfall CDF (Cumulative Distribution Function) of historical model and observation values. Srivastav et al. (2014) applied equidistance-quantile matching technique for updating rainfall IDF curves at four locations in Canada fitting GCM annual maximum rainfall and sub-daily observed data. Ogarekpe (2014) compared rainfall IDF curves derived from three models, including exponential, logarithmic and power models for Calabar, Nigeria. Their study indicates that the logarithmic model best produces intensity values compared to the observations and is appropriate for applying to design of hydraulic structures.

This study predicts rainfall IDF curves using spatial and temporal downscaled GCM data. Overall, objective of this research is to assess climate change impact on rainfall IDF curves in Hanoi, Vietnam. The assessment of climate change impacts on rainfall IDF curves includes the following major steps: (i) extraction of multiple GCM participation output over the Hanoi station for different emission scenarios; (ii) bias correction of GCM rainfall output for current and future climate periods; (iii) derivation of short-duration rainfall intensities for different return periods; and (iv) development and comparative analysis of rainfall IDF curves. Multiple GCM and scenarios were used to reflect the uncertainty associated climate change. Daily rainfall output of 5 GCM (ACCESS1-0, GFDL-CM3, GFDL-ESM2G, MRI-CGCM3.2 and NoESM1-M) was used for the climate change impact assessment. Representative Concentration Paths (RCP) 4.5 and 8.5 indicating medium and high greenhouse emission scenarios were considered for the study (IPCC 2014). Quantile mapping technique enabled to correct the biases in the GCM rainfall data. The simple scaling method was applied to derive annual maximum 15 min, 30 min, 1 h, 1.5 h, 2 h, 4 h, 8 h and 12 h rainfall intensities for each of the year over 1976–2005 (current) and 2070–2099 (future) periods. Finally, using frequency analysis, 2-, 5-, 10-, 25, 50- and 100 years rainfall IDF curves were developed for current and future climate. The chapter will provide an insight to the water planners and managers to re-examine urban development processes for municipal water and wastewater services by visualizing climate change impacts on infrastructure design, capital investment projects, service planning, and operation and maintenance (Saraswat et al. 2017; Saraswat and Kumar 2016). This study is an attempt to quantify the potential effects of climate change (specifically for precipitation) and using the rainfall characteristics to design robust water infrastructures and sustainable management.

6.2 Study Area and Data Collection

6.2.1 Study Area

The study area is capital city Hanoi, Vietnam, which is also a political and economic center of the country. Hanoi is located at 21°01′N and 105°51′E. The topography of Hanoi is very diverse with three main terrain zones, including the delta, hills and mountains; the delta accounts for over 80% area of the city. The river system in and around Hanoi city consists of many tributary rivers of the Red River and the Thai Binh River basin system. The river system is mainly characterized as sloping with narrow riverbeds and complicated meanders. Therefore, the capacity to drain water away is quite low. Specifically, when heavy rainfall occurs, it can cause a significant rise in the river level. The annual mean temperature in the central delta of Hanoi is approximately 23–24 °C and in the mountain zones it is slightly lower. The temperature difference between the hottest and coldest months is relatively large; the highest temperature is greater than 28 °C in the summer and the lowest temperature is less than 18 °C in the winter. The amount of annual rainfall in this area ranges

from 1400 mm to 2000 mm. The rainy season in the city extends from the middle of April to the end of October. The total rainfall during the rainy season accounts for more than 80% of the annual rainfall. The average annual number of rainy days is approximately 150, of which there are 7 to 8 days when daily rainfall is over 50 mm and 1–2 days when daily rainfall is over 100 mm per day. Extremely heavy rainfall sometimes occurs in the first 2 months of the winter. Heavy rainfall events in 1984, 1996 and 2008, caused serious inundation in the study area.

6.2.2 Data Collection

6.2.2.1 Observation Data

In this study, daily rainfall observations from the Hanoi station covering the period of 1961–2005 were collected for bias correction of the GCM output. In addition, rainfall data of several short duration extreme events were collected from this station. The dataset consists of rainfall in several durations including 15 min, 30 min, 1 h, 1.5 h, 2 h, 4 h, 8 h and 12 h. Both daily and shorter-duration rainfall datasets are provided by the Vietnam institute of meteorology, hydrology and climate change.

6.2.2.2 GCM Data

There are a number of GCM and emission scenarios, providing predictions of future changes in climate. Due to a great amount of uncertainty associated with the scenarios and projections, use of multiple GCM is recommended to provide the range of recommendations for addressing various climate change impacts. Various studies are available to select GCM and scenarios. Broadly, future climateprojections are defined by four greenhouse emission scenarios withone mitigation scenario (RCP 2.6), two medium stabilization scenarios (RCP 4.5/RCP 6) and one very high baseline emission scenario (RCP 8.5). The RCP 2.6 scenario is considered largely idealistic as world leaders have not yet reached toconsensus emission mitigation strategies towards restricting this level. Climate projections for RCP 4.5 and RCP8.5 emission sceanarios, which represent medium stabilization scenario and the high emission scenario and cover most likely range of radiative forcing, were considered for estimating future rainfall extremes. Tens of GCMs have been developed globally for these emission scenarios. McSweeney et al. (2015) compared rainfall characteristics of various CMIP5 (Coupled Model Intercomparison Project Phase 5) GCMs to identify a set of 8–10 suitable GCMs across multiple regions: Southeast Asia, Europe and Africa. Accordingly, rainfall output of 5 GCMs with RCP 4.5 and RCP 8.5 emission scenarios were selected for analysing climate change impact on extreme rainfall over Hanoi. Table 6.1 provides brief description of Information about these models are described in Table 6.1 below, which is edited for this study based on the report issued by CSIRO and Bureau of Meteorology (2015).

Table 6.1 Information of CMIP5 models using in this study

CMIP5 Model ID	Institute and Country of Origin	Atmosphere horizontal resolution (°Lat × °Lon)	Historical	RCP4.5	RCP8.5
ACCESS1-0	CSIRO, Australia	1.9 × 1.2	1961–2005	2070–2099	
GFDL-CM3	NOAA, USA	2.5 × 2.0			
GFDL-ESM2G					
MRI-CGCM3	MRI, Japan	1.1 × 1.1			
NorESM1-M	NCC, Norway	2.5 × 1.9			

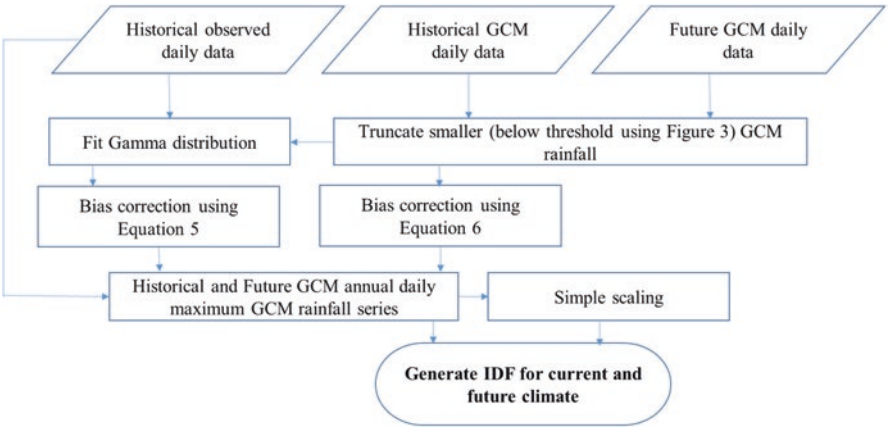

Fig. 6.1 Framework for generating rainfall IDF curves under climate change

6.3 Methodology

There are two major components under the research methodology (Fig. 6.1). These are statistical downscaling and establishment of rainfall IDF curves for different return periods. Bilinear interpolation and conventional quantile mapping bias correction techniques were applied for the spatial downscaling. The simple scaling method was applied for the temporal downscaling. Short durations rainfall intensities for various return periods were derived using Gumbel distribution.

6.3.1 Downscaling

6.3.1.1 Spatial Downscaling

Spatial downscaling consisted of two major steps. These are interpolation and bias correction of GCM rainfall output. Various methods are available for interpolating scanty data. Inverse weighted distance, Thiessen polygon and bilinear techqunique are popular interpolation technique to address coarse resolution resolution data

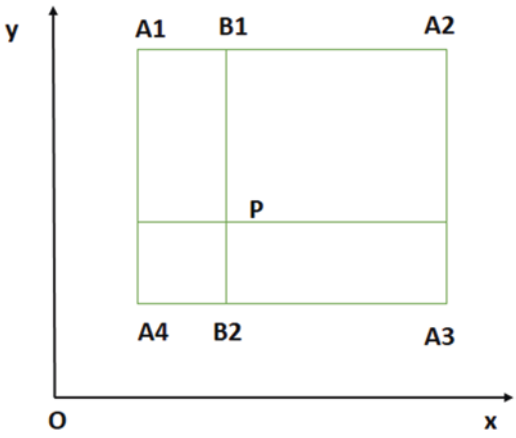

Fig. 6.2 The bilinear interpolation method

problem. Bilinear interpolation is widely used for gridded time series from RCM or GCM output (WaSiM 2012; Sluiter 2009; Yuan et al. 2016). The gridded data are treated as station data by considering four nearest quadrants. In this method, distance-weighted average of the four nearest values is used to estimate a new value. Geographical location of observation rainfall station and surrounding GCM grid cells are required to calculate their distances from the observation station. Accordingly, GCM data was derived from grid points. In Fig. 6.2, A1, A2, A3 and A4 are four nearest point around the interest point P. The interpolation in x direction is performed at first to derive B1 and B2. Then, another in y direction is carried out to obtain the value at the desired point P.

Climate outputs from GCM is usually not the same as the climate from observations. Hence, GCM rainfall outputs without performing some form of bias correction are not suggested for climate change impact assessments (Sharma et al. 2007; Hansen et al. 2007). Bias correction is applied to derive realistic GCM outputs by comparing and establishing a relationship between climate model outputs and observations at a station. Quantile mapping technique enabled to minimize the rainfall frequency and intensity bias in GCM data. In the beginning, problem of excessive rainy days are corrected by truncating GCM rainfall below a threshold value. This threshold value is estimated by comparingnon-exceedance probability of zero rainfall value in the observation and GCM rainfall data series (Fig. 6.3). Later, truncated values are adjusted by applying inverse CDF of the GCM data with observational shape and scale parameters. Threhold values estimated at monthly scale were applied for correcting GCM rainfall data.

The gamma PDF (Probability Density Function) and CDF can be expressed by the Eqs. (6.1) and (6.2), respectively; the shape and scale parameters can be calculated by functions (6.3) and (6.4), respectively.

$$f(x) = \frac{1}{\beta^{\alpha}\Gamma(\alpha)} x^{\alpha-1} e^{-x/\beta} \tag{6.1}$$

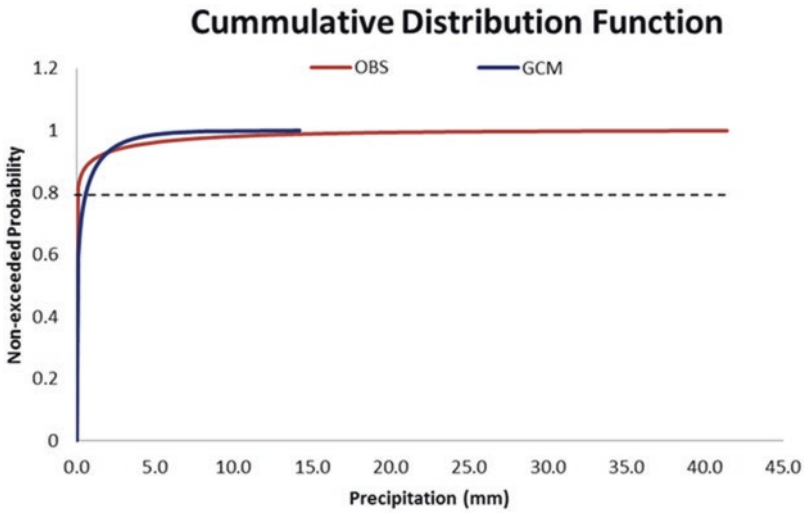

Fig. 6.3 Determining the threshold value for frequency correction, Hanoi during 1961–1975. (Note: OBS is observed value)

$$F(x) = \int_{x}^{0} f(t)\,dt \tag{6.2}$$

$$\alpha = \left(\frac{\overline{x}}{\sigma}\right)^2 \tag{6.3}$$

$$\beta = \frac{\sigma^2}{\overline{x}} \tag{6.4}$$

where x is daily rainfall, $\overline{x}$ is mean and σ is standard deviation of considered data series. Equations (6.5) and (6.6) illustrate the transformation of the bias correction method to match GCM rainfall distribution with observation rainfall distribution for baseline and future periods, respectively. The corrected GCM rainfall for the baseline period was estimated by calculating the inverse CDF of the GCM, with shape and scale parameters from the observation dataset. In terms of the future correction, a scaling factor was added by taking the ratio of the inverse CDF of future GCM rainfall to the observational and baseline GCM rainfall distribution parameters.

$$x_{GCM_{baseline-corrected}} = F_{obs}^{-1}\left[F_{GCM_{baseline-raw}}\left(x_{GCM_{baseline-raw}}\right)\right] \tag{6.5}$$

$$x_{GCM_{future-corrected}} = x_{GCM_{future}} \frac{F_{obs}^{-1}\left[F_{GCM_{future}}\left(x_{GCM_{future}}\right)\right]}{F_{GCM_{baseline}}^{-1}\left[F_{GCM_{future}}\left(x_{GCM_{future}}\right)\right]} \tag{6.6}$$

where, F is CDF and F^{-1} is its inverse.

In this study, we chose period of 1976–2005 as baseline period. At first, quantile-mapping technique was applied to remove systematic bias for this baseline. Later, the method is also employed to correct bias for an independent period covering 15 years from 1961 to 1975. We chose this period for independent testing of Eq. 6.6 because of the limit in observation and model historical simulation.

6.3.1.2 Temporal Downscaling

High-temporal-resolution (e.g., 15 min, 30 min, and 1-h) data are needed to create the IDF curves. Since the available data are available at daily intervals, it is necessary to temporally downscale the daily maximum rainfall intensity to hourly or sub-hourly rainfall intensities for different return periods. For the purpose of constructing rainfall IDF curves for the future period, scaling theory was applied to produce short-duration rainfall intensity of daily rainfall data. The scaling property is proven by many studies and is applied to rainfall intensity by Menabde et al. (1999), Nhat et al. (2007), and Mishra and Herath (2011). Scaling properties of extreme rainfall are analyzed for different durations as due to significant variation in statistical moments over different durations. Scaling approach enables to derive data from coarse temporal resolution to fine resolution. This way scaling technique helps to derive hourly extreme rainfall from daily values. Based on empirical analysis, Menabde et al. (1999) proposed that random variable I_d and I_D representing annual maximum rainfall intensities over d and D *time duration* respectively can have the following relationship (Eq. 6.7).

$$I_d = \left(\frac{d}{D}\right)^{-\eta} I_D \tag{6.7}$$

The equality and η in Eq. 6.7 refers to identical probability distribution function and scaling exponent respectively. The relationship between the moments of order q can be obtained by raising both sides of equation to power q and taking the expected values of both sides (Eq. 6.8).

$$E\left[I_d^q\right] = \left(\frac{d}{D}\right)^{-\eta(q)} E\left[I_D^q\right] \tag{6.8}$$

Estimation of scaling exponent η includes (i) log-log graph of moments $E\left[I_D^q\right]$ *versus* durations of different order q; and (ii) linear graph of slopes (*of moments versus duration lines*) and moment order q. If the resulting graph is a straight line i.e., value of η (slope) remains same for different values of q, it is of simple scaling otherwise it is of multi-scaling.

6.3.2 Rainfall IDF Curves Construction

The rainfall IDF curve is constructed by using short-durations rainfall observations from the Hanoi station. The Gumbel distribution is chosen for conducting frequency analysis. The cumulative distribution function can be expressed as below:

$$F_d(i) = exp\left(-exp\left(-\frac{i-\mu_d}{\sigma_d}\right)\right) \tag{6.9}$$

where, $\boldsymbol{i}$ is rainfall intensity, $\boldsymbol{\mu_d}$ and $\boldsymbol{\sigma_d}$ are the location and scale parameters respectively, and $\boldsymbol{F_d(i)}$ is the non-exceedance probability of intensity $\boldsymbol{i}$ in duration $\boldsymbol{d}$.

To obtain the rainfall intensity i from a given probability or return period, we find the inverse of function (6.9) by taking the natural logarithm of the left side twice. After doing this step, function (6.10) is derived:

$$i = \mu_d - \sigma_d * \left(ln\left(-ln\left(\mathbf{1}-\frac{\mathbf{1}}{T}\right)\right)\right) \tag{6.10}$$

where, T is the return period. The relationship between the return period T and the non-exceedance probability $\boldsymbol{F_d}$ is shown in function (6.11):

$$T = \frac{\mathbf{1}}{\mathbf{1}-F_d} \tag{6.11}$$

6.4 Results and Discussion

6.4.1 Validation of Quantile-Mapping Technique

Figure 6.4 shows the comparison between the monthly observed total rainfall from 1976 to 2005 and the five bias-corrected GCM results as well as their average number of monthly rainy days The quantile mapping technique produces total rainfall estimates which are very close to the observations in every month of the year. Furthermore, in terms of frequency calibration, this bias correction method is obviously accurate. The best performance of frequency bias correction method is shown for ACCESS1-0 and NorESM1-M. However, there is a small difference between the number of observed rainy days and from the bias corrected GCM outputs. There are 3–5 more and sometime fewer days than observations. Overall, the bias correction method produces good results in adjusting rainfall from raw GCM outputs, specifically in the amount of rainfall for dependent period.

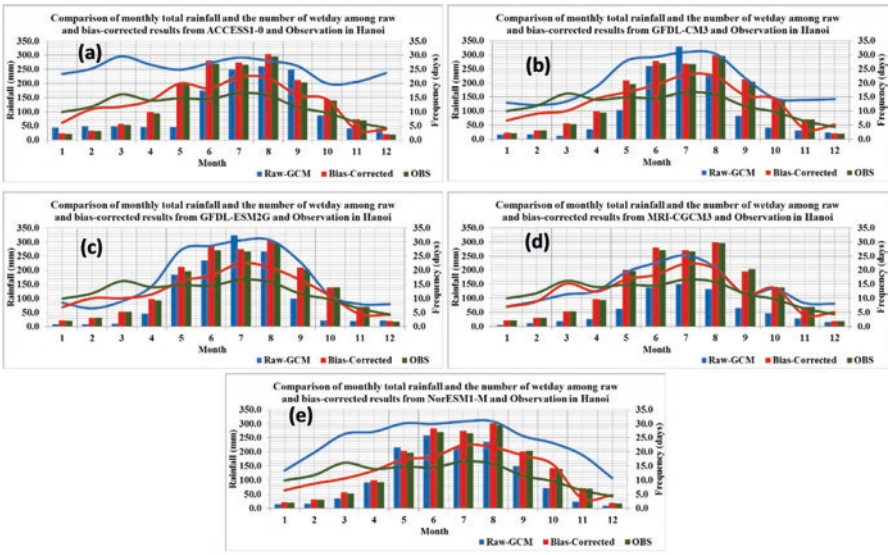

Fig. 6.4 Comparison of monthly total rainfall (column) and the number of wet days (line) among bias corrected GCM (red), raw GGMs (blue) and Observation (green) for period of 1976–2005; (**a**) ACCESS1-0, (**b**) GFDL-CM3, (**c**) GFDL-ESM2G, (**d**) MRI-CGCM3, (**e**) NorESM1-M

Quantile mapping performed well in predicting the amount of rainfall and the number of rainy days. In addition, it also performs well in capturing extreme events at the Hanoi station base on Q-Q plots of rainfall greater than the 95th percentile (Fig. 6.5). The most rainfall extreme values obtained from bias corrected models are relatively close to observations. For the highest value, three models including GFDL-CM3, MRI-CGCM3 and NorESM1-M show better fit than other models.

We also examined performance of bias correction technique for an independent period of 1961–1975 in order to assess the ability to apply it for removal of model bias for future period. For the annual cycle, rainfall, it is indicated from Fig. 6.6 that monthly total rainfall is improved significantly after eliminating systematic bias for instance in the summer. Specifically, the efficiency of bias correction technique is much clearer for September to November. The amount of rainfall in these 3 months range from 50 mm to around 250 mm meanwhile rainfall from raw GCM such as GFDL-CM3, GFDL-ESM2G and MRI-CGCM3 is usually around 100 mm. The adjusted result captures very well this characteristic. It is also similar to the number of wet days that bias – corrected method produces frequency of rainy days with higher agreement to observation. For extreme value (Fig. 6.7), bias correction method also performs conducive skill in matching raw GCM output to observation, specifically for the MRI-CGCM3 model. For other models, the two highest values are quite larger than previous observation. In summary, quantile – mapping demonstrates an advance skill in removal of bias for an independent period.

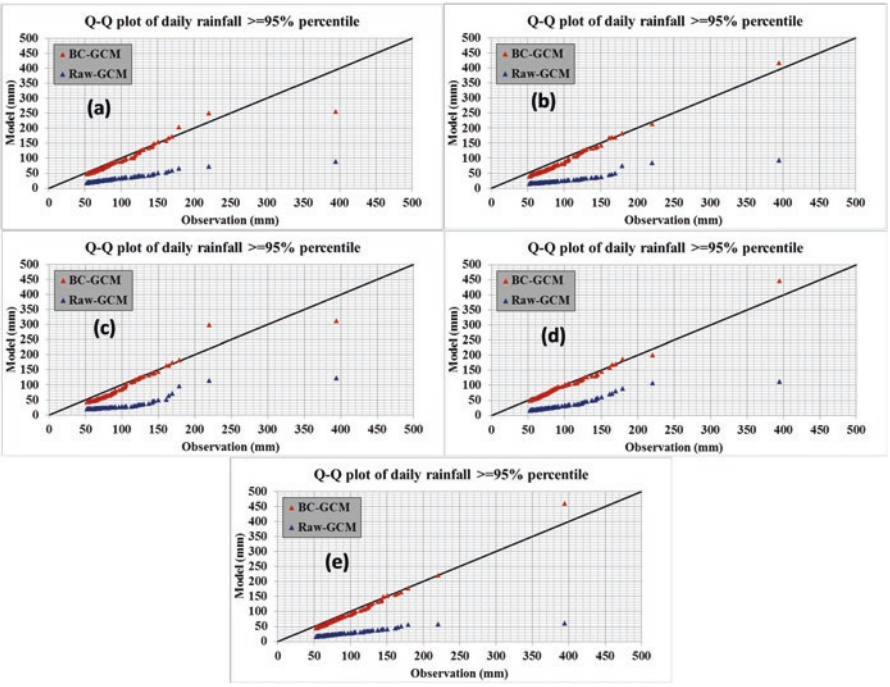

Fig. 6.5 Q-Q plot comparing rainfall greater than 95th percentile from bias corrected GCM and Observation (Red) and comparing raw GCM and Observation (blue) for period 1976–2005; (**a**) ACCESS1-0, (**b**) GFDL-CM3, (**c**) GFDL-ESM2G, (**d**) MRI-CGCM3, (**e**) NorESM1-M

6.4.2 Rainfall Intensity – Duration – Frequency Curves

Table 6.2 and Fig. 6.8 show rainfall intensity for nine different durations and six return periods at the Hanoi station. This result is obtained by using the Gumbel distribution for frequency analysis of observational short-duration rainfall datasets from 1976 to 2005. For the 100-year return period, average rainfall intensity in 15 min is 206 mm/h, in 1 h is 148.3 mm/h and in 24 h is 18.7 mm/h. There was one time that heavy rain with the amount of rainfall greater than 18.7 occurred, in 1984. For the 25-year return period, rainfall intensities are 175.4 mm/h, 121.3 mm/h and 14.5 mm/h in 15 min, 1 h and 24 h, respectively. For the 2-year return period, rainfall intensity in 15 min is 113.5 mm/h. The corresponding rainfall intensity in 1 h and 24 h are 66.6 and 6.1 mm/h, respectively.

For future rainfall IDF (Figs. 6.9 and 6.10), results from five GCM were combined by finding the ensemble mean. Rainfall intensity for different durations and return periods under both RCP4.5 and RCP8.5 scenarios are presented in Tables 6.3 and 6.4. These results indicate that rainfall intensity under RCP4.5 may increase much more than RCP8.5 for most durations and return periods. For the 100-year return period, rainfall intensity increases 42.6% in comparison with the baseline

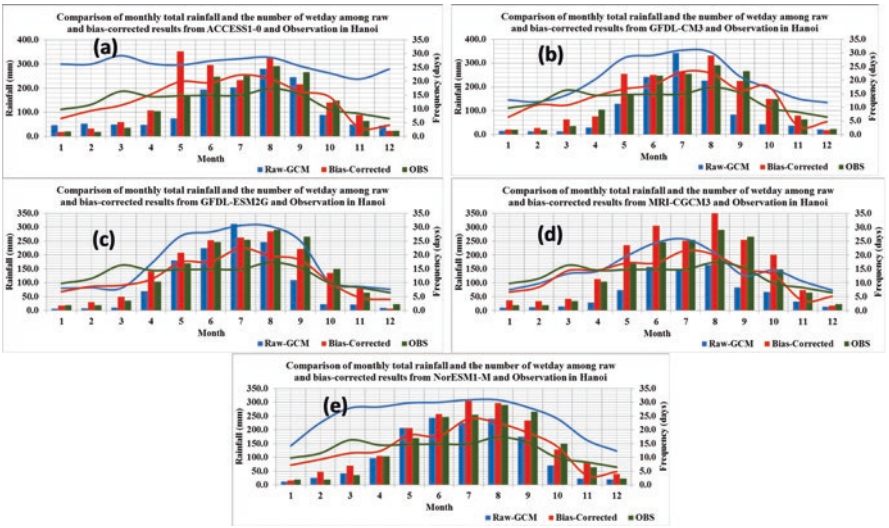

Fig. 6.6 Comparison of monthly total rainfall (column) and the number of wet days (line) among bias corrected GCM (red), raw GGMs (blue) and Observation (green) for independent period of 1961–1975; (**a**) ACCESS1-0, (**b**) GFDL-CM3, (**c**) GFDL-ESM2G, (**d**) MRI-CGCM3, (**e**) NorESM1-M

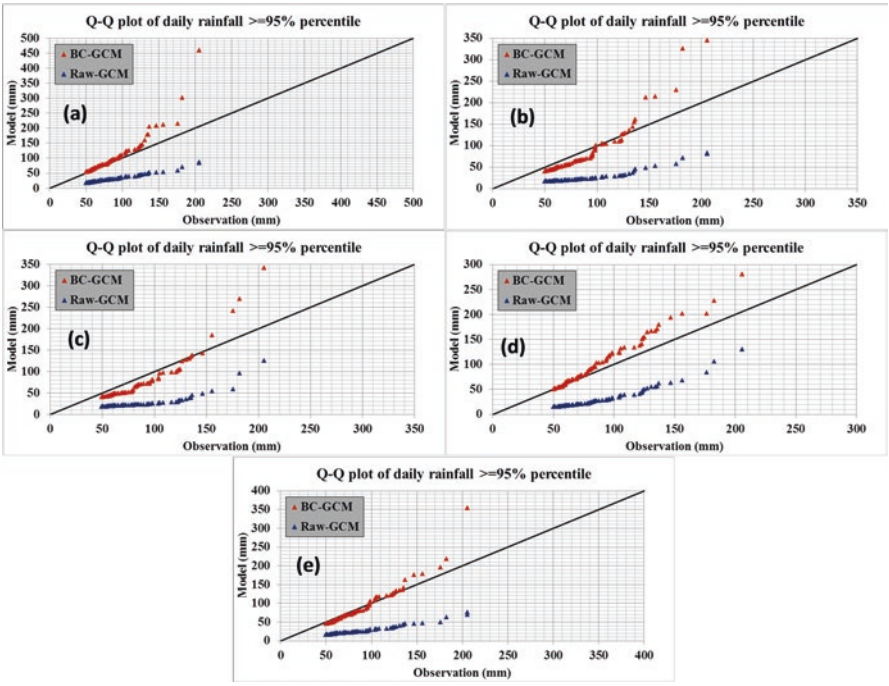

Fig. 6.7 Q-Q plot comparing rainfall greater than 95th percentile from bias corrected GCM and Observation (Red) and comparing raw GCM and Observation (blue) for independent period 1916–1975; (**a**) ACCESS1-0, (**b**) GFDL-CM3, (**c**) GFDL-ESM2G, (**d**) MRI-CGCM3, (**e**) NorESM1-M

period under RCP4.5. The corresponding increasing value under RCP4.5 is 38.8%. This implies that by the end of century, heavy rain may occur with extremely high intensity under both scenarios. However, the frequency of this event is very rare. For the 2-year return period, in 15 min, rainfall intensity increases 5.4% under RCP8.5 and up to 7.2% under RCP4.5. With this amount of increase, total rainfall after 15 min may be 121 mm and 119.6 mm by the end of century under RCP4.5 and RCP8.5, respectively.

6.5 Conclusions

In this chapter, the study argued that for sustainable urban planning and effective urban water management the analysis of future rainfall and its extreme events is very useful in order to design strong infrastructure and reduce flood risks and climatic vulnerability. For the same, the study developed the rainfall IDF curve to evaluates the impact of climate change on extreme rainfall intensities under medium and high greenhouse gases emission (RCP 4.5 and RCP 8.5 respectively) for the future period of 2070–2099 over a baseline of 1976–2005 using rainfall output of 5

Table 6.2 Rainfall intensity in several durations (D) and return periods (T) from observation for 1976–2005

T (↓)D(→)	15’	30’	1 h	1.5 h	2 h	4 h	8 h	12 h	24 h
2 years	113.5	90.5	66.6	49.3	40.3	23.2	13.7	10.2	6.1
5 years	138.2	116.2	88.5	65.8	54.6	32.4	20.3	15.1	9.5
10 years	154.6	133.3	103.0	76.8	64.1	38.5	24.6	18.4	11.7
25 years	175.4	154.8	121.3	90.6	76.0	46.2	30.1	22.6	14.5
50 years	190.7	170.7	134.8	100.8	84.9	51.9	34.2	25.6	16.7
100 years	206.0	186.5	148.3	111.0	93.7	57.5	38.2	28.7	18.7

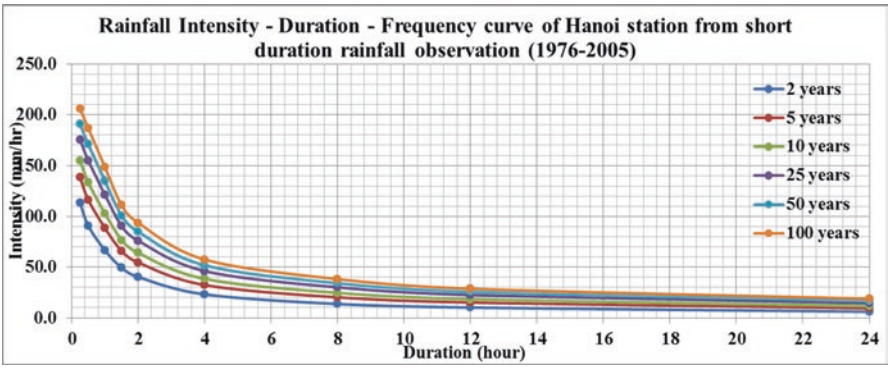

Fig. 6.8 Rainfall IDF curve of Hanoi station from observation data for 1976–2005

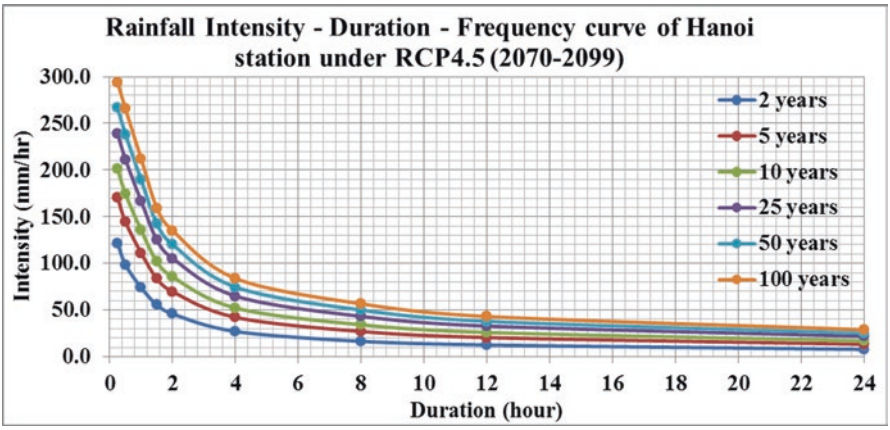

Fig. 6.9 Rainfall IDF Curve of Hanoi station for 2070–2099 under RCP4.5

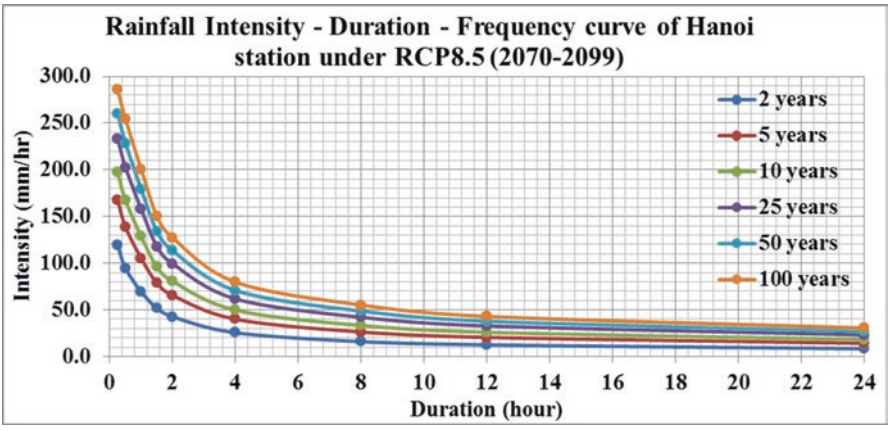

Fig. 6.10 Rainfall IDF curve of Hanoi station for 2070–2099 under RCP8.5

Table 6.3 Change of rainfall intensity in several durations (D) and return period (T) by the end of century under RCP4.5

T (↓), D (→)	15'	30'	1 h	1.5 h	2 h	4 h	8 h	12 h	24 h
2 years	7.2	8.8	11.0	12.4	13.8	16.8	20.6	23.4	28.4
5 years	23.4	24.2	25.6	26.8	27.6	30.2	33.4	35.8	40.0
10 years	30.2	30.8	31.6	32.6	33.4	35.6	39.0	40.8	45.0
25 years	36.2	36.6	37.4	38.0	38.6	40.8	43.6	45.4	49.4
50 years	39.8	39.6	40.4	41.2	41.6	43.8	46.2	48.0	52.0
100 years	42.6	42.4	43.0	43.4	44.2	45.8	48.2	50.2	54.0

Table 6.4 Change of rainfall intensity in several durations (D) and return period (T) by the end of century under RCP8.5

T (↓), D (→)	15'	30'	1 h	1.5 h	2 h	4 h	8 h	12 h	24 h
2 years	5.4	4.4	4.2	5.0	6.0	10.2	17.2	23.2	38.0
5 years	21.4	19.4	19.0	19.2	20.0	23.6	30.0	35.6	50.0
10 years	27.6	25.6	25.0	25.0	25.8	29.2	35.4	40.8	54.6
25 years	33.2	31.0	30.2	30.2	30.8	33.8	39.8	45.4	58.8
50 years	36.6	34.0	33.0	33.2	33.6	36.4	42.6	47.8	61.4
100 years	38.8	36.4	35.4	35.4	35.8	38.6	44.4	49.8	63.2

GCM. The bilinear interpolation and quantile mapping were applied and observational data is used to correct the bias of GCM simulations. The results of the research are of significant practical importance of design, operation, and maintenance of stormwater management, flood risk management, rainwater harvesting and water-related infrastructures in the capital city of Vietnam, Hanoi. It indicated that the methodology used accurately capture extreme values of rainfall for all 5 GCM and by the end of the century, rainfall intensity may increase in all durations and return periods under both RCP 4.5 and RCP 8.5 scenarios. Also, the results indicated that the mean of corrected monthly rainfall and the frequency of wet days are considerably closer to observation than the raw rainfall estimates. In addition, the bias correction method accurately captured extreme rainfall values for all 5 GCM and point out that by the end of the century, under different scenarios the rainfall intensity is increasing for all the duration and the return periods.

The results support the argument that the urban water management should be an integral part of sustainable urban development planning and development of rainfall IDF curves is very important in designing the sustainable water system, effective water management and sustainable urban infrastructures. The developed IDF curves are extremely useful in the sustainable development planning of the Hanoi, Vietnam, this will help the urban planners, local policymakers and water managers in designing sustainable water infrastructures such as stormwater infrastructure, storage structures, rainwater harvesting structures, flood management solutions and others. From the policy perspective, the developed rainfall IDF curves assist the local policymakers and urban planners to understand and visualize the future impacts of extreme rainfall events and climate change on current infrastructure and provides an opportunity for informed decisions. This helps the inclusion of the strong stormwater facilities, flood management, robust and sustainable water urban infrastructure in urban development policies.

Acknowledgement This study was supported by the United Nations University – Institute for the Advanced Study of Sustainability, Tokyo. We would also like to thank the Asia Pacific Network for Global Change Research (APN) for financially supporting under Project ARCP2015-20NMY-Mishra: Climate Change Adaptation through Optimal Stormwater Capture Measures: Towards a New Paradigm for Urban Water Security.

Reference

Adusumalli M, Arora K (2015) Towards sustainable community and institutional response to climate extremes: a situational analysis of institutions, communities and their response to climate change induced disasters in Uttarakhand. Euro Sci J Spec Edn, pp 66–86

Akpan SU, Okoro BC (2013) Developing rainfall intensity–duration–frequency models for Calabar City, south-south, Nigeria. Am J Eng Res (AJER) 02(06):19–24

Bernard MM (1932) Formulas for Rainfall Intensities of Long Durations. Trans ASCE 96:592–624

Chakraborty S, Chakraborty A (2017) Satoyama landscapes and their change in a River Basin context: lessons for sustainability. Issues Soc Sci 5(1):38–64. https://doi.org/10.5296/iss.v5i1.10892

Conca K (2006) The new face of water conflict, vol 3. Woodrow Wilson International Center for Scholars, Washington, DC

Connor R (2015) The United Nations world water development report 2015: water for a sustainable world, vol 1. UNESCO Publishing, Paris

CSIRO and Bureau of Meteorology (2015) Climate change in Australia information for Australia's natural resource management regions: technical report, CSIRO and Bureau of Meteorology, Australia

De Paola F, Giugni M, Topa ME, Bucchignani E (2014) Intensity-duration-frequency (IDF) rainfall curves, for data series and climate projection in African cities. SpringerPlus 3:133. https://doi.org/10.1186/2193-1801-3-133

Hanjra MA, Qureshi ME (2010) Global water crisis and future food security in an era of climate change. Food Policy 35(5):365–377

Hansen JW, Challinor A, Ines A, Wheeler T, Moron V (2007) Translating climate forecasts into agricultural terms: advances and challenges. Clim Res 33(1):27–41

Hatt BE, Fletcher TD, Deletic A (2007) Treatment performance of gravel filter media: implications for design and application of stormwater infiltration systems. Water Res 41(12):2513–2524

IPCC (2014) Climate change 2014: synthesis report. Contribution of Working Groups I, II and III to the fifth assessment report of the Intergovernmental Panel on Climate Change. IPCC, Geneva. pp 151

Jago-on KAB, Kaneko S, Fujikura R, Fujiwara A, Imai T, Matsumoto T, …, Taniguchi M (2009) Urbanization and subsurface environmental issues: an attempt at DPSIR model application in Asian cities. Sci Total Environ 407(9):3089–3104

Kuo CC, Gan TY, Gizaw M (2015) Potential impact of climate change on intensity duration frequency curves of central Alberta. Clim Chang 130:115. https://doi.org/10.1007/s10584-015-1347-9

Le MN, Tachikawa Y, Takara K (2006) Establishment of intensity-duration-frequency curves for precipitation in the monsoon area of Vietnam. Ann Disaster Prev Res Inst Kyoto Univ, No. 49 B, 2006

Logah F, Kankam-Yeboah K, Bekoe E (2013) Developing short duration rainfall intensity frequency curves for Accra in Ghana. Int J Latest Res Eng Comput (IJLREC) 1:67–73

Mai KN, Herath S (2014) Urban water balance recovery by network of distributed rain-water infiltration and storage facilities–Case study of Japanese urban catchment. United Nations University. Retrieved October 30, 2017, from https://www.researchgate.net/profile/Ngoc_mai_Kim/publication/291957259_Urban_water_balance_recovery_by_network_of_distributed_rain-water_infiltration_and_storage_facilities_-_Case_study_of_Japanese_urban_catchment

McSweeney CF, Jones RG, Lee RW, Rowell DP (2015) Selecting CMIP5 GCMs for downscaling over multiple regions. Clim Dyn 44:3237–3260. https://doi.org/10.1007/s00382-014-2418-8

Menabde M, Seed A, Pegram G (1999) A simple scaling model for extreme rainfall. Water Resour Res 35(1):335–339

Mirhosseini G, Srivastava P, Stefanova L (2012) The impact of climate change on rainfall intensity-duration-frequency (IDF) curves in Albama. Reg Environ Chang. https://doi.org/10.1007/s10113-012-0375-5

Mishra BK, Herath S (2011) Rainfall intensity duration frequency curves under climate change scenario in urban Kathmandu valley. NEA-JC Newslett 6(2):19–22

Mishra BK, Herath S (2014) Assessment of future floods in the Bagmati River basin of Nepal using Bias-corrected daily GCM precipitation data. J Hydrol Eng. https://doi.org/10.1061/(ASCE)HE.1943-5584.0001090

Mishra BK, Regmi RK, Masago Y, Fukushi K, Kumar P, Saraswat C (2017) Assessment of Bagmati River pollution in Kathmandu Valley: scenario-based modeling and analysis for sustainable urban development. Sustain Water Qual Ecol 9:67–77

Mpelasoka FS, Chiew FHS (2009) Influence of rainfall scenario construction methods on runoff projections. J Hydrometeorol 10(5):1168–1183

Nguyen V-T-V, Nguyen T-D, Cung A (2007) A statistical approach to downscaling of sub-daily extreme rainfall processes for climate-related impact studies in urban areas. Water Sci Technol Water Supply 7(2):183–192

Nhat LM, Tachikawa Y, Sayama T, Takara K (2007) Regional rainfall intensity duration-frequency relationships for ungauged catchments based on scaling properties. Ann Disaster Prev Res Inst Kyoto Univ 50B:33–43

Ogarekpe NM (2014) Development and comparison of different intensity duration frequency models for Calabar, Nigeria. Niger J Technol (NIJOTECH) 33(1):33–42

Pereira LS, Cordery I, Iacovides I (2009) Coping with water scarcity: addressing the challenges. Springer, Dordrecht

Prodanovic P, Simonovic SP (2007) Development of rainfall intensity duration frequency curves for the city of London under the changing climate. Water Resour Res Rep, London

Rodríguez R, Navarro X, Casas MC, Ribalaygua J, Russo B, Pouget L, Redaño A (2014) Influence of climate change on IDF curves for the metropolitan area of Barcelona (Spain). Int J Climatol 34:643–654. https://doi.org/10.1002/joc.3712

Saraswat C, Kumar P (2016) Climate justice in lieu of climate change: a sustainable approach to respond to the climate change injustice and an awakening of the environmental movement. Energy Ecol Environ 1(2):67–74

Saraswat C, Kumar P, Mishra BK (2016) Assessment of Stormwater Run-off Management Practices and Governance under climate change and urbanization: an analysis of Bangkok, Hanoi and Tokyo. Environ Sci Policy 64:101–117

Saraswat C, Mishra BK, Kumar P (2017) Integrated urban water management scenario modeling for sustainable water governance in Kathmandu Valley, Nepal. Sustain Sci, 1–17

Sharma D, Das Gupta A, Babel MS (2007) Spatial disaggregation of bias-corrected GCM precipitation for improved hydrologic simulation: ping river basin, Thailand. Hydrol Earth Syst Sci 11(4):1373–1390

Sluiter R (2009) Interpolation methods for climate data: literature review, KNMI intern rapport:IR 2009-04, The Netherlands

Srivastav RK, Schardong A, Simonovic SP (2014) Equidistance quantile matching method for updating IDF curves under climate change. Water Resour Manag 28:2539–2562

Takeuchi K, Brown RD, Washitani I, Tsunekawa A, Yokohari M (eds) (2003) Satoyama: the traditional rural landscape of Japan. Springer, New York

Tremblay H (2010) A clash of paradigms in the water sector? Tensions and synergies between integrated water resources management and the human rights-based approach to development. Tensions and Synergies Between Integrated Water Resources Management and the Human Rights-Based Approach to Development (August 1, 2010)

UNDESA-United Nations Development of Economic and Social Affairs (2016) International decade for action 'water for life' 2005–2015. http://www.un.org/waterforlifedecade/scarcity.shtml

UNEP (2012) The UN-Water Status Report on the Application of Integrated Approaches to Water Resources Management. Available from: www.unwater.org/rio2012/report

US Environmental Protection Agency – EPA (2015) Stormwater Best Management Practices (BMP) Performance Analysis. Boston, US: EPA. http://www.epa.gov/climatechange/basics. Accessed on 11th of August, 2015

Wang X, Huang G, Liu J (2014) Projected increases in intensity and frequency of rainfall extremes through a regional climate modeling approach. J Geophys Res Atmos 119:13,271–13,286. https://doi.org/10.1002/2014JD022564

WaSim (2012) Water balance Simulation Model (WaSim), Hydrology Software Consulting, J. Schulla Regensdorferstrasse 162 CH 8049 Zürich

Westra S, Fowler HJ, Evans JP, Alexander LV, Berg P, Johnson F, Kendon EJ, Lenderink G, Roberts NM (2014) Future changes to the intensity and frequency of short duration extreme rainfall. Rev Geophys 52:522–555

Willems P, Vrac M (2011) Statistical precipitation downscaling for small-scale hydrological impact investigations of climate change. J Hydrol 402:193–205. https://doi.org/10.1016/j.jhydrol.2011.02.030

Yan T, Wang J, Huang J (2015) Urbanization, agricultural water use, and regional and national crop production in China. Ecol Model 318:226–235

Yilmaz AG, Hossain I, Perera BJC (2014) Effect of climate change and variability on extreme rainfall intensity–frequency–duration relationships: a case study of Melbourne. Hydrol Earth Syst Sci 18:4065–4076

Yuan F, Ma M, Ren L, Shen H, Li Y, Jiang S, Yang X, Zhao C, Kong H (2016) Possible future climate change impacts on the hydrological drought events in the Weihe River Basin, China. Advances in Meteorology. https://doi.org/10.1155/2016/2905198